Journal of Cell Science 113, 4533-4543 (2000)
Printed in Great Britain © The Company of Biologists Limited 2000
JCS1878

Yeast myosin light chain, Mlc1p, interacts with both IQGAP and Class II myosin to effect cytokinesis

James R. Boyne[1,*], Hirzun Mohd Yosuf[1,*,‡], Pawel Bieganowski[2,*], Charles Brenner[2] and Clive Price[1,§]

[1]Krebs Institute for Biomolecular Research, Department of Molecular Biology and Biotechnology, University of Sheffield, PO Box 594, Western Bank, Sheffield S10 2TN, UK
[2]Kimmel Cancer Institute, Thomas Jefferson University, 233 South 10th Street, Philadelphia PA 19107, USA
*These authors contributed equally to this work
‡Present address: Fakulti Sains dan Bioteknologi, Universiti Pertanian Malaysia, 43400 UPM Serdang, Selangor Darul Ehsan, Malaysia
§Author for correspondence (e-mail: clive.price@sheffield.ac.uk)

Accepted 5 October; published on WWW 16 November 2000

SUMMARY

***MLC1* (myosin light chain) acts as a dosage suppressor of a temperature sensitive mutation in the gene encoding the *S. cerevisiae* IQGAP protein. Both proteins localize to the bud neck in mitosis although Mlc1p localisation precedes Iqg1p. Mlc1p is also found at the incipient bud site in G_1 and the growing bud tip during S and G_2 phases of the cell cycle. A dominant negative GST-Mlc1p fusion protein specifically blocks cytokinesis and prevents Iqg1p localisation to the bud neck, as does depletion of Mlc1p. These data support a direct interaction between the two proteins and immunoprecipitation experiments confirm this prediction. Mlc1p is also shown to interact with the class II conventional myosin (Myo1p). All three proteins form a complex, however, the interaction between Mlc1p and Iqg1p can be separated from the Mlc1p/Myo1p interaction. Mlc1p localisation and maintenance at the bud neck is independent of actin, Myo1p and Iqg1p. It is proposed that Mlc1p therefore functions to recruit Iqg1p and in turn actin to the actomyosin ring and that it is also required for Myo1p function during ring contraction.**

Key words: Yeast, Myosin light chain, IQGAP, Cytokinesis

INTRODUCTION

Cytokinesis, the partitioning of the cytosol, is the final step in the mitotic cell cycle. In animal cells cytokinesis is effected via the formation of an actomyosin contractile ring leading to the formation of the cleavage furrow. The positioning of this ring and timing of contraction are precisely regulated and co-ordinated with nuclear and/or mitotic spindle position and mitosis (Glotzer, 1997). However, details of the regulation of cytokinesis remain to be thoroughly elucidated. Recent evidence has established that budding yeast, *Saccharomyces cerevisiae*, also utilizes an actomyosin contractile ring during cytokinesis (Lippincott and Li, 1998a; Bi et al., 1998). These studies have created the possibility of using a genetic approach to understand both the formation and function of the contractile ring. In order to address these issues it is first necessary to identify all structural and regulatory components of the contractile ring. Recently several novel proteins have been implicated in the regulation of cytokinesis in budding yeast, e.g. Akr1p and Hof1p/Cyk2p (Kao et al., 1996; Kamei et al., 1998; Lippincott and Li, 1998b). A third protein Iqg1p/Cyk1p (hereafter termed Iqg1p) was identified by homology with mammalian IQGAP proteins. Null mutations were shown to lead to a failure in cytokinesis, although this phenotype is strain dependent (Epp and Chant, 1997; Lippincott and Li, 1998a; Osman and Cerione, 1998). IQGAP proteins appear to be composites of a number of functional domains originally characterised in other polypeptides and these include a calponin homology domain (CH), a RasGAP homology domain (GRD) and a so called IQ domain. Consistent with the identification of these domains Iqg1p has been shown to interact with a variety of different cytoskeletal associated proteins which include actin, Cdc42p, Tem1p and Cmd1p (Epp and Chant, 1997; Osman and Cerione, 1998; Shannon and Li, 1999). There remain differences in the literature with respect to Cdc42p binding, an interaction originally suggested by two hybrid analysis but one which has not been supported by in vitro binding studies (Osman and Cerione, 1998; Shannon and Li, 1999).

IQ domains were originally defined as myosin light chain binding sites and are situated between the head and tail domains of all myosin heavy chain molecules (Cheney and Mooseker, 1992; Xie et al., 1994). Myosin light chains are members of the EF-hand super family of Ca^{2+} binding proteins, one member of which is calmodulin. Calmodulin has been shown to act as a light chain partner for both vertebrate and yeast myosin V (Espindola et al., 1992; Brockerhoff et al., 1994). Myo2p, a budding yeast myosin V, localises to sites of polar growth during the cell division cycle and is thought to play a role in vesicle movement (Lillie and Brown, 1994; Johnston et al., 1991; Govindan et al., 1995). Myosin light chain binding to the heavy chain plays both structural and

regulatory roles in myosin function (Xie et al., 1994; Fromherz and Szent-Gyorgi, 1995). Recently the calmodulin related Mlc1p (myosin light chain) has been identified as a second light chain which interacts with Myo2p (Stevens and Davis, 1998). Iqg1p contains five tandemly arrayed IQ domains suggesting that this protein also interacts with members of the EF-hand protein super-family.

Here we report the isolation of a temperature sensitive allele of *IQG1* which we have termed *iqg1-1* and demonstrate that *MLC1* acts as a dosage suppressor of this mutation. We present a cytological analysis of the *iqg1-1* phenotype demonstrating that the primary defect lies in cytokinesis and that other reported cellular defects are secondary to this. A dominant negative *mlc1* allele blocks cytokinesis and these cells fail to accumulate Iqg1p at the bud neck. Mlc1p is shown to localise to the incipient bud site and bud tip during early bud growth and subsequently to a ring structure at the bud neck, at the point of the metaphase to anaphase transition. Furthermore, co-immunoprecipitation experiments demonstrate that Mlc1p and Iqg1p are physically associated in mitosis. The class II myosin, Myo1p, is shown to interact with both Mlc1p and Iqg1p. These data allow the further elaboration of a model for the sequential assembly of the cytokinetic machinery at the bud neck.

MATERIALS AND METHODS

Yeast strains, methods and media

The yeast strains used in this study were of the W303 background and are listed in Table 1. Growth was in YPD (1% yeast extract, 2% bactopeptone, 2% glucose) at the stated temperature. Plasmid containing strains were propagated on selective synthetic medium (Sherman, 1991). Experiments requiring galactose for induction of gene expression were carried out in selective synthetic medium containing 2% galactose. Solid medium made to the same recipes contained 2% agar. Yeast plasmid transformations with exception of the library screens were carried out by a rapid colony procedure (Keszenman-Pereyra and Hieda, 1988) and all other yeast transformations by a standard lithium acetate method (Ito et al., 1983). DNA was prepared by a standard spheroplast protocol (Philippsen et al., 1991). G_0 cells were obtained following the inoculation of exponentially growing cells into either YPD or synthetic medium containing either 0.2% glucose or 0.2% galactose, growth was continued for 48 hours at which point all cells were unbudded and uninucleate. S phase arrest was achieved by the addition of 10 mM hydroxyurea (HU) to exponentially growing cultures. Arrest was maintained for 180 minutes before release by washing in 10 volumes of pre-warmed, fresh YPD and growth then continued in 1 volume of medium. Depolymerisation of F-actin was carried out in the presence of 200 μM latrunculin A (from a 16 mM stock in DMSO).

Stain construction

All primers used are listed in Table 2.

Primers CLI12 and 13 were used to introduce a triple-HA tag linked to *Kluveromyces lactis TRP1* gene at the C terminus of *MLC1* using the plasmid pWZ89 as a template, using standard PCR and site specifc recombination methodology (Wach et al., 1994). The heterozygous diploid IQG1*/iqg1-1* (SSC189) was used as the host strain and linkage of the insert to the *MLC1* locus was tested using primers CLI14 and 15 which lie 5′ and 3′ to the site of insertion to generate a diagnostic 1.3 kbp fragment. Two positive transformants were sporulated and the segregation of tryptophan prototrophy shown to be 2:2. Following sporulation *IQG1* and *iqg1-1* haploids carrying the *MLC1-3HA* allele were isolated (SSC215 and SSC228). The same approach was employed to tag *IQG1* using primers CLI16 and 17 to amplify the 3HA-*TRP1* cassette and primers CLI18 and 19 to identify positive transformants. Segregation of the *TRP1* marker was analyzed after sporulation and shown to be 2:2 and haploid strains (SSC225 and SSC229) were selected. Using the same primers we amplified a c-myc epitope cassette using pWZ87 as the template and performed the same targeting protocol. In this case we failed to recover viable haploids after segregation but were able to demonstrate linkage of *TRP1* to the *iqg1-1* allele. *MYO1* was tagged with nine c-myc (9E10) epitopes in the same manner using primers CLI114 and CLI115. In all of the above procedures PCR reactions were carried out in pre-mixed 50 μl volumes and 30 cycles with parameters of 30 seconds denaturation at 94°C, 1 minute annealing at 48°C and 2 minutes extension at 72°C were performed. Five independent reactions were pooled, ethanol precipitated and the DNA dissolved in 10 μls H_2O prior to use in yeast transformation. The following standard genetic crosses were then used to generate the haploid strains used in this study; 842-1 × SSC215 –

Table 1. Yeast strains

Strain	Genotype	Source
SSC1	*MAT **a** ade2.1 leu2-3,112 his3-5 trp1-1 ura3-52 can1-100*	Laboratory Collection
SSC2	*MAT α ade2-1 leu2-3,112 his3-5 trp1-1 ura3 can1-100*	Laboratory Collection
SSC18	*MAT **a** cdc15-1 ade2-1 leu2-3,112 his3-5 trp1-1 ura3-52 can1-100*	Laboratory Collection
SSC166	*MAT **a** iqg1-1 ade2-1 leu2-3,112 his3-5 trp1-1 ura3 –52 can1-100*	This study
SSC167	*MAT α iqg1-1 ade2-1 leu2-3,112 his3-5 trp1-1 ura3 –52 can1-100*	This study
SSC189	*MAT **a**/MATα IQG1/iqg1-1ade2-1/ade2-1 leu2-3,112 /leu2-3,112 his3-5 /his3-5 trp1-1/trp1-1 ura3 –52 /ura3 –52 can1-100/can1-100*	This study
SSC215	*MAT **a** MLC1-3HA::TRP1 ade2-1 leu2-3,112 his3-5 trp1-1 ura3 –52 can1-100*	This study
SSC216	*MAT **a** MLC1-3HA::TRP1 iqg1-1 ade2-1 leu2-3,112 his3-5 trp1-1 ura3 –52 can1-100*	This study
SSC218	*MAT **a** MLC1-3HA::TRP1 cdc15-1 ade2-1 leu2-3,112 his3-5 trp1-1 ura3 –52 can1-100*	This study
SSC225	*MAT **a** IQG1-3HA::TRP1 ade2-1 leu2-3,112 his3-5 trp1-1 ura3 –52 can1-100*	This study
SSC226	*MAT **a** IQG1-3HA::TRP1 cdc15-1 ade2-1 leu2-3,112 his3-5 trp1-1 ura3-52 can1-100*	This study
SSC228	*MATα MLC1-3HA::TRP1 ade2-1 leu2-3,112 his3-5 trp1-1 ura3 –52 can1-100*	This study
SSC229	*MATα IQG1-3HA::TRP1 ade2-1 leu2-3,112 his3-5 trp1-1 ura3 –52 can1-100*	This study
SSC239	*MAT **a** iqg1-1-3HA::TRP1 ade2-1 leu2-3,112 his3-5 trp1-1 ura3 –52 can1-100*	This study
SSC255	*MAT **a** MYO1-9Myc:TRP1 IQG1-3HA::TRP1 cdc15-1 ade2-1 leu2-3, 112 his3-5 trp1-1 ura3-52 can1-100*	This study
SSC267	*MAT **a** MYO1-9Myc:TRP1 cdc15-1 ade2-1 leu2-3, 112 his3-5 trp1-1 ura3-52 can1-100*	This study
SSC349	*MAT **a** myo1::URA3 MLC1-3HA::TRP1 ade2-1 leu2-3,112 his3-5 trp1-1 ura3 –52 can1-100*	This study
SSC350	*MAT **a** myo1::URA3 IQG1-3HA::TRP1 ade2-1 leu2-3,112 his3-5 trp1-1 ura3 –52 can1-100*	This study
SSC351	*MAT **a** iqg1-1-3HA::TRP1 MYO1-9Myc:TRP1 ade2-1 leu2-3,112 his3-5 trp1-1 ura3 –52 can1-100*	This study
SSC353	*MAT **a** mlc1::KanMX LEU2::GAL-MLC1 ade2-1 leu2-3,112 his3-5 trp1-1 ura3 –52 can1-100*	This study
SSC354	*MAT **a** mlc1::KanMX LEU2::GAL-MLC1 IQG1-3HA::TRP1 ade2-1 leu2-3,112 his3-5 trp1-1 ura3 –52 can1-100*	This study
MPK1-3HA	*MAT **a** MPK1-3HA::TRP1 ade2-1 leu2-3,112 his3-5 trp1-1 ura3 –52 can1-100*	P. Sudbery

Table 2. Deoxyoligonucleotide primers

CLI12	5′GCAACGGAGAAATTGACTACAAGAAGTTCATCGAAGATGTTTTGAGACAATCCGGTTCTGCTGCTAG 3′
CLI13	5′TAGGACTCTGTTATATAGTAATAAATGTCTAAATTTGCAGTTCCGCACTCTCACCTCGAGGCCAGAAGAC 3′
CLI14	5′AGACGAGCTGTTGAAGGGT 3′
CLI16	5′GCCAATTACTACATTTGATTGTCAGTTTTTTTCTATAAAAGGAACGCTTTGTCCGGTTCTGCTGCTAG 3′
CLI17	5′AATTTAGTAACAGCTTTTGCCCAATATGCTCAAAACCGAGTTATCTATTACCTCGAGGCCAGAAGAC 3′
CLI18	5′GAAATTATTCCATTCCAACGT 3′
CLI19	5′GCTGCTGAAAATAAGGAAAAT 3′
CLI20	5′GGATCCATGTCAGCCACCAGAGCCA 3′
CLI35	5′CCCCGGGTTGTCTCAAAACATCTTCGATGAA 3′
CLI114	5′GATAGGCTCGAAAAATATTGATAGTAACAATGCACAGAGTAAAATTTTCAGTTCCGGTTCTGCTGCTGCTAG 3′
CLI115	5′TAAATAAAGGATATAAAGTCTTCCAAATTTTTAAAAAAAAGTTCGTTACCTCGAGGCCAGAAGAC 3′

SSC223; JP7A × SSC227 – SSC223; SSC18 × SSC227 – SSC218; SSC167 × SSC215 – SSC216; SSC229 × SSC018 – SSC226; SSC353 × SSC229 – SSC354.

In order to create a *mlc1* null mutant, a copy of wild-type *MLC1* under control of the *GAL1* promoter was integrated at the *LEU2* locus in a diploid. One copy of the *MLC1* open reading frame was deleted using pFA6-kanMX4 as a template to amplify a G418 resistance marker flanked by sequences immediately 5′ and 3′ to the *MLC1* coding region. Selected diploids were sporulated and *LEU2*, G418 resistant haploids isolated on galactose containing medium. All selected haploids were unable to grow on glucose rich medium and the *mlc1* deletion structure confirmed by PCR analysis with primers 5′ to the site of integration. One such haploid (SSC353) was used for further studies. The *myo1* null mutants (SSC350 and SSC351) were constructed by a combination of standard PCR and cloning techniques and the entire *MYO1* open reading frame was replaced with *URA3* by targeted integration, details available on request.

Plasmid and DNA manipulations

Primers CLI 20 and 35 were used to amplify the *MLC1* open reading frame which was then inserted into pPCR-Blunt (Invitrogen). The correct orientation of insert was identified by *Bam*HI digestion which linearises the appropriate plasmid. The wild-type DNA sequence was confirmed, using PE Applied Biosystems BigDye™ terminator Sequencing reagents and protocols and samples analysed on an Applied Biosystems Model 373A DNA Sequencing System. The gene was then excised as a 490 bp *Bam*HI/*Xho*I fragment and subcloned into the 2 μm plasmid pEG-KT (Mitchell et al., 1993) pGST-MLC1. The *MLC1* plasmids shown in Fig. 2 were constructed by sub-cloning the following DNA fragments from the original suppressor plasmid. pHAD1 carries a 2.813 kbp *Bam*HI/*Sph*I fragment encoding *MLC1* and *ARC1* inserted between the cognate sites in the polylinker of Ycplac33. The pHAD2 plasmid carries a 2.238 kbp *Hin*dIII/*Bgl*II fragment inserted between the *Hin*dIII and *Bam*HI sites of the same polylinker. pHAD3 is derived from pHAD1 by deletion of a restriction fragment lying between two *Kas*I sites, one within *MLC1* and the other in the vector sequence.

The wild-type and mutant *IQG1* loci were sequenced following genomic PCR using a primer walking strategy and the primer sequences are available on request (from C. J. Brenner).

Escherischia coli strain DH5α was used as a host for all bacterial transformations which were carried out by electroporation (Calvin and Hanawalt, 1988). Bacterial GST-Mlc1p was affinity purified on glutathione-agarose beads (Sigma) and eluted in 5 mM reduced glutathione (Sigma) according to standard methods (Smith and Johnson, 1988). Poly-clonal anti-sera were raised in Dwarf lop rabbits after sub-cutaneous injection of the bacterial fusion protein in the presence of Freund's adjuvant (Harlow and Lane, 1988).

Immunofluorescence

Cells were fixed in growth medium by adding 37% formaldehyde to a final concentration of 3.7% and incubating at room temperature for 1 hour. All cells were treated with zymolyase after fixation to remove the cell wall and then sonicated. 1 ml of fixed cells were washed twice in solution B (100 mM K_2HPO_4, 100 mM KH_2PO_4, 1.2 M Sorbitol) and then incubated for 15-30 minutes in 1 ml of solution B + 1 μg zymolyase 20T (ICN Biomedicals Inc.) and 2 μl of 2-mercaptoethanol. Cells were examined under a Nikon light microscope to ensure that the cell wall had been removed, then washed twice in solution B before resuspending in 100 μl of solution B. Staining of the *IQG1-HA* and *MLC1-HA* strains with mouse anti-HA (BAbCO) primary antibody and TRITC-conjugated or FITC-conjugated secondary antibodies (Jackson Immunoresearch) was carried out as described (Ayscough and Drubin, 1998). Phalloidin staining was performed as described (Adams and Pringle, 1991). When co-staining cells with both anti-HA and phalloidin the methanol/acetone step was removed. After the secondary antibody incubation was complete, cells were incubated with 0.05 mM rhodamine-phalloidin (Fluka BioChemika) in the dark for 30 minutes. All cells were visualized using a Leica DMRB microscope fitted with a RTE/CCD-1800-V CCD camera (Princeton Instruments). Image analysis was carried out using Openlab software vs2.06 (Improvision).

Interaction by co-immunoprecipitation

Strains SSC18, SSC218 and SSC226 were grown overnight in 25 ml of YPD at 26°C. These cultures were shifted to 37°C by adding an equal volume of YPD, pre-warmed to 48°C and grown for a further two hours at 37°C to arrest cell division. Cells were pelleted, washed once in 1 ml of PBS and then in 1 ml of lysis buffer (50 mM Tris-base, 50 mM NaF, 5 mM EDTA, 1 mM DTT, 80 mM β-Glycerolphosphate, 15 mM nitrophenolphosphate, 25 mM NaCl, 0.1 mM sodium orthovanadate, 1% v/v NP40, 40 μg/ml pepstatin A, 40 μg/ml aprotinin, 20 μg/ml leupeptin, 200 μg/ml PMSF). The cells were then pelleted and the supernatant discarded, two volumes of acid washed glass beads were added to the pellet and further lysis buffer was added to cover the glass beads. Tubes were then placed in a Ribolyser (Hybaid) and agitated (3× 10 seconds) and then placed immediately on ice. The supernatant was collected after low speed centrifugation at 2000 rpm for 2 minutes and then transferred to a new tube and centrifuged at 14000 rpm for a further 5 minutes at 4°C. Protein concentrations were determined by Bradford assay (Bradford, 1976). The experiments described in Fig. 5 used 1 mg of total protein in all immunoprecipitations (IP) in a total volume of 500 μl. In contrast experiments using asynchronous cultures (Fig. 6B,C,D) 5 mg of total protein was used. In all immunoprecipitations 1 μl of either anti-HA monoclonal (BAbCO), monoclonal anti-Myc (BAbCO) or anti-GST-Mlc1p polyclonal was added to the protein extract and incubated at 4°C with mixing for one hour. Protein-G beads (50 ml of a 50% slurry, Sigma) were then added to each IP and incubated for a further hour at 4°C with mixing. The beads were pelleted by centrifugation at 2500 rpm, the supernatant removed and the beads washed five times in 1 ml of lysis buffer. SDS-PAGE loading buffer (50 mM Tris-HCl, 100 mM DTT, 2% SDS, 0.1% bromophenol blue, 10% glycerol) was added to the beads after the final wash and the samples boiled for five minutes, centrifuged at 14000 rpm for three minutes and the supernatant then loaded onto either a 6% or 12% SDS-PAGE gel (BioRad Mini-Protean II) and proteins separated at a

constant 120 V until the dye front reached the bottom of the gel. Pre-stained protein markers (New England Biolabs) were also loaded. Proteins were then transferred to Hybond-C nitrocellulose membrane (Amersham) using a wet-blotting system (Bio-Rad Trans-Blot Cell) and western transfer buffer (25 mM Tris-HCl, 192 mM glycine, 20% methanol). Immunoblot analysis was performed using the enhanced chemiluminescence kit (Amersham) and Hyperfilm MP (Amersham) according to the manufacturer's instructions. Anti-HA (16B12 monoclonal antibody, BAbCO) was used at a dilution of 1:4000 followed in by anti-mouse-HRP (DAKO) diluted 1:4000. The anti-GST-Mlc1p polyclonal was used at a dilution of 1:6000 and followed in by anti-rabbit-HRP (DAKO) diluted 1:4000. Anti-c-myc (9E10 monoclonal antibody, BAbCO) was used at a dilution of 1:4000 followed in by anti-mouse-HRP (DAKO) diluted 1:4000.

RESULTS

Isolation of the *iqg1-1* allele

In the course of a synthetic lethal screen designed to identify genes which interact with *HNT2*, the *S.cerevisiae* homologue of the putative human tumour suppressor gene, FHIT (Brenner et al., 1999) we uncovered one candidate mutation which exhibited temperature sensitive growth at 37°C. Subsequent genetic analysis demonstrated that this mutation was not synthetically lethal in combination with an *hnt2*::*TRP1* null mutation (data not shown). The mutation was backcrossed three times and in these and in all subsequent crosses it behaved as a single, recessive point mutation exhibiting 2:2 segregation of a conditional cytokinesis defect. Fifteen complementing plasmids were isolated from a centromeric plasmid library (ATCC 77162) and eight of these carried the *IQG1* locus. We subsequently sequenced the mutant *iqg1-1* locus and found a single T-C transition leading to a Leu-Pro alteration at amino acid 457. We confirmed that the parent strain carried the wild-type *IQG1* sequence. Segregation analysis of a backcross followed by DNA sequencing of all four haploid progeny of a tetrad (segregating 2:2 for temperature sensitivity) revealed that the mutation was coincident with the conditional cytokinesis phenotype (data not shown). In order to demonstrate linkage between the mutation and the *IQG1* locus we epitope tagged the *iqg1-1* allele resulting in the introduction of a *TRP1* marker at the site of integration. The tagged mutant was then crossed to an *IQG1* strain and a segregation analysis performed. Temperature sensitive growth and tryptophan prototrophy always co-segregated, 18 tetrads scored, demonstrating linkage between the mutation and the introduced *TRP1* marker. Finally sub-cloning of *IQG1* alone into a centromeric plasmid fully complemented the mutation. Taken together these data indicate that we have isolated a temperature sensitive allele of *IQG1* (Epp and Chant, 1997; Lippincott and Li, 1998a) and that the Leu457Pro substitution within Iqg1p confers a cytokinesis defective phenotype.

Phenotypic analysis of *iqg1-1* mutants

Characterisation of the terminal *iqg1-1* phenotype revealed that cells carrying the mutation failed to complete cytokinesis and grew as chains of cells often containing multinucleate compartments (Fig. 1A). Neither sonication nor cell wall removal caused cells to separate demonstrating that the defect is in cytokinesis and not cell separation. Previous work had indicated that *iqg1* null mutants were defective in cytokinesis

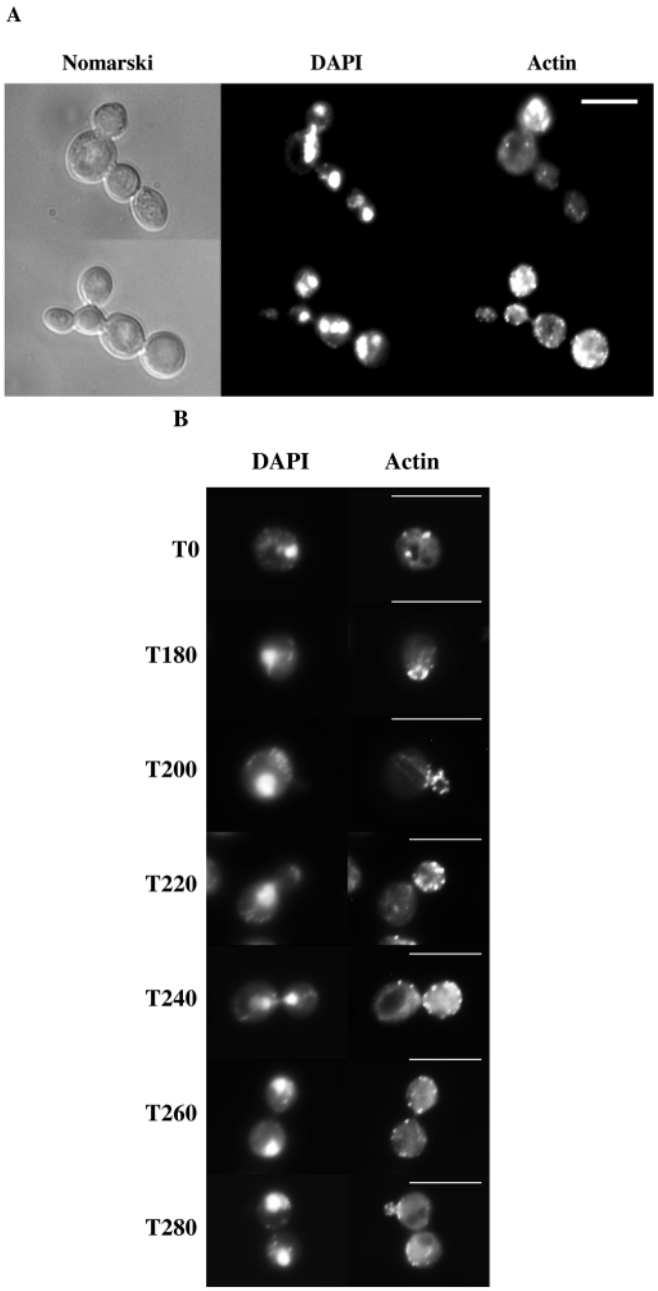

Fig. 1. Characterisation of the *iqg1-1* mutation. (A) Mutant cells, SSC166, were grown at 26°C in YPD and shifted to 37°C for six hours. Cells were fixed in 3.7% formaldehyde and stained with DAPI and rhodamine-conjugated phalloidin. The left panel shows the Nomarski image of typical cell morphology. The central panel illustrates the nuclear distribution and the right panel actin localisation. Bar, 10 μm. (B) Synchronous release of G_0 *iqg1-1* cells. Mutant cells were innoculated into fresh YPD at 37°C, fixed in formaldehyde at the indicated time points and stained to characterise the nuclear cycle (left panel) and actin distribution (right panel). Bar, 10 μm.

(Epp and Chant, 1997; Lippincott and Li, 1998a). More recently published results suggested that *iqg1* deficient cells were unable to undergo normal polar growth (Osman and Cerione, 1998). Whilst these data probably reflect differences in the strain backgrounds used it was important to re-address

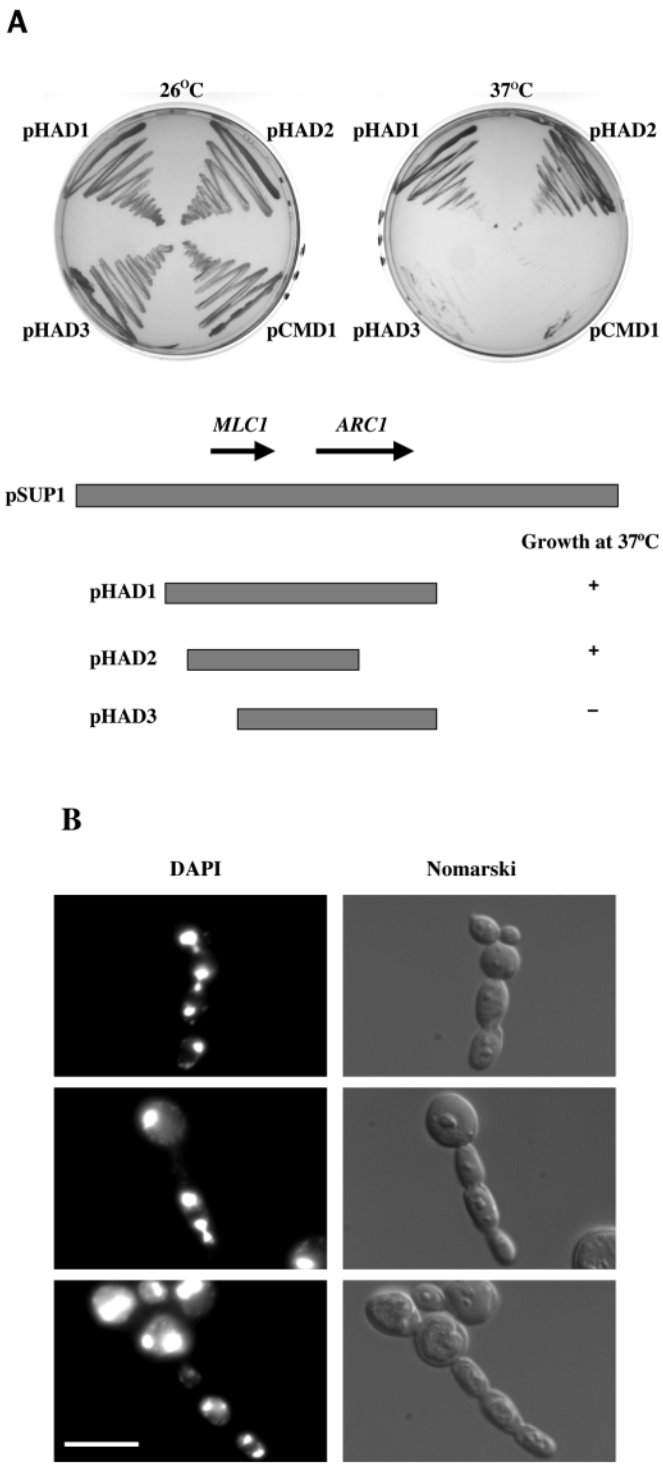

Fig. 2. *MLC1* suppression of the *iqg1-1* mutation, (A) The original *MLC1* library fragment and centromeric plasmid subclones are illustrated. Suppression of temperature sensitive growth, strain SSC166, by those plasmids containing an intact *MLC1* is also shown. In contrast a high copy number plasmid carrying *CMD1* does not permit growth at the restrictive temperature. (B) Dominant negative GST-Mlc1p. Starvation synchronised cells were released into fresh selective medium containing galactose to induce expression of the GST-Mlc1p fusion protein. Cells are able to undergo polarised cell growth but fail to complete cytokinesis; examples are shown of cells fixed and stained between 4 and 6 hours after release. Bar, 10 μm.

the issue utilising the unique *iqg1-1* allele. Cytological analysis of *iqg1-1* cells synchronised at START by nutritional limitation and released into fresh growth medium at the restrictive temperature revealed that the first cycle proceeds normally until cytokinesis (Fig. 1B). Subsequently the cells exhibit isotropic actin and chitin distribution suggesting that these are indirect consequences of a failure in cytokinesis (Fig. 1A and data not shown). Moreover, multinucleate cell compartments do not accumulate in the first cycle, indicating that nuclear movement and mitotic spindle formation are normal. This was consistent with the observation of normal spindle staining (data not shown). To test whether the block to cytokinesis arose as a result of a failure of actomyosin ring formation we also examined actin localisation in synchronous *iqg1-1* cells at the restrictive temperature (Fig. 1B). In a control wild-type culture we observe 19% (n=100) of late anaphase cells (t=260 minutes) with actin localized to the ring. At the same time point 14% (n=100) of mutant, *iqg1-1*, cells contain an actin ring at the bud neck at the permissive temperature whereas we never observe actin ring staining in *iqg1-1* cells at the restrictive temperature. However, there is clear evidence of polarised actin localisation to the growing bud in the earlier time points illustrating that the altered pattern of actin staining is specific to the bud neck at a late stage in the cell cycle. Indeed in the final time point there is polarisation of actin to the new bud despite the loss of Iqg1p function and the failure of cytokinesis.

MLC1 acts as a dosage suppressor of *iqg1-1*

In a separate complementation experiment with a second centromeric plasmid borne genomic library (Rose et al., 1987) we isolated one plasmid dependent suppressor of *iqg1-1*. DNA sequencing and deletion mapping indicated that this suppressor corresponded to the *MLC1* locus (Fig. 2A). Targeted integration at the *MLC1* locus in an *iqg1-1* background and subsequent genetic analysis demonstrated that the two loci were unlinked (data not shown). Further genetic analysis confirmed that *MLC1* exhibits haplo-insufficiency and that null mutants were defective in cytokinesis, in agreement with previous data (Stevens and Davis, 1998). Plasmid borne *MLC1* failed to suppress an *iqg1* deletion mutation demonstrating that the observed suppression of the *iqg1-1* allele was not due to a bypass mechanism. The fact that Mlc1p and calmodulin, encoded by *CMD1* (Davis et al., 1986), are known to interact with Myo2p via the IQ domain led us to test whether multi-copy *CMD1* was able to suppress the *iqg1-1* mutation. The data in Fig. 2A clearly demonstrate that multi-copy CMD1 does not permit growth of an *iqg1-1* strain at the restrictive temperature. Microscopic observation of the cells at 37°C confirmed that the *iqg1-1* phenotype remains unaltered (not shown).

Dominant negative Mlc1p inhibits cytokinesis

We constructed an N-terminal glutathione-S-transferase fusion to Mlc1p (GST-Mlc1p) under galactose dependent transcriptional control. Cells were synchronised at START and released into selective medium containing galactose. The data show that bud emergence and the first cell cycle continue as in wild type but that at later time points cytokinesis is not completed and multi-nucleate chains of cells begin to accumulate (Fig. 2B). These chains remain after cell wall removal and sonication indicating that they do not result from a failure of cell separation. The appearance of these cells is also

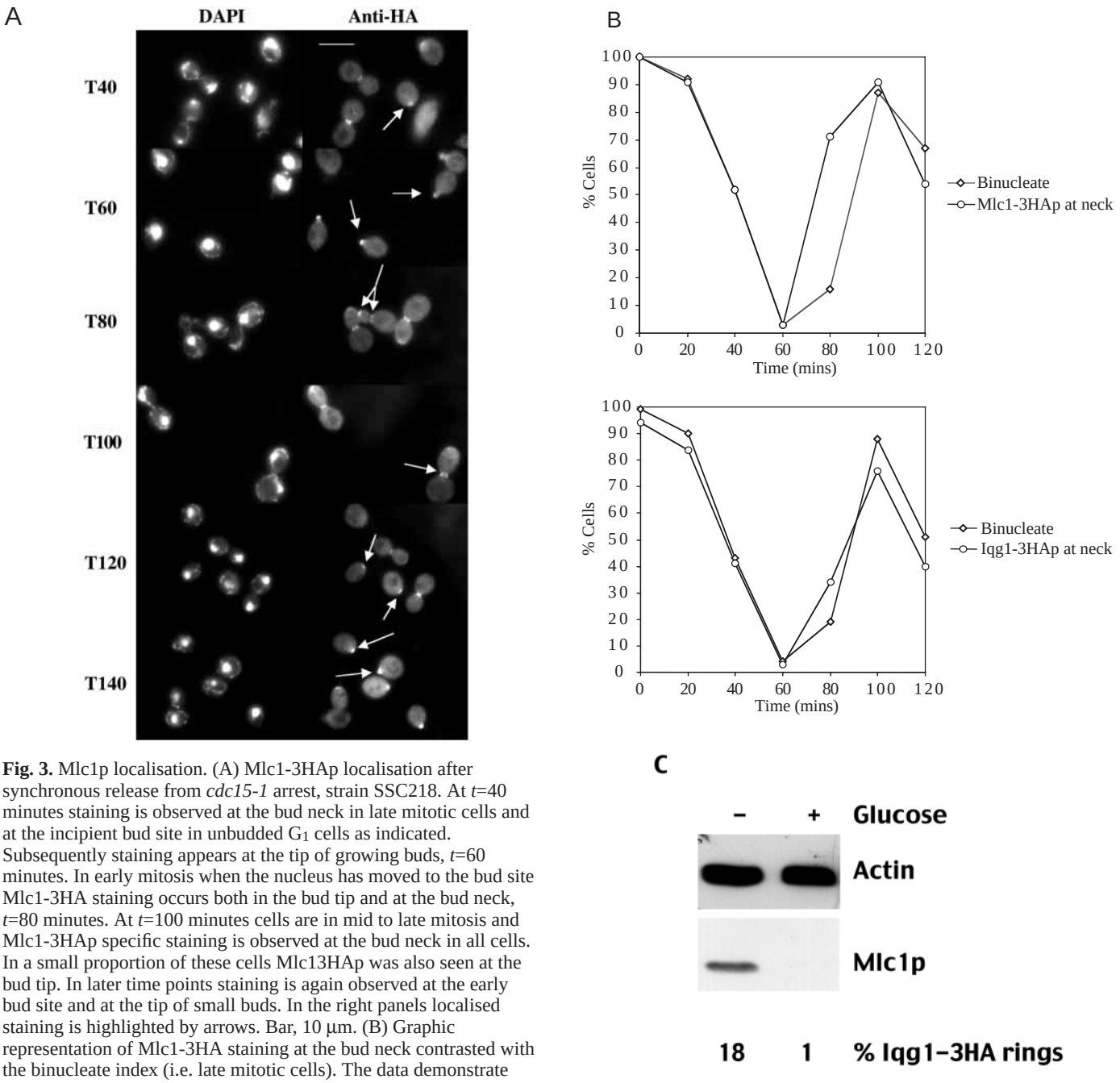

Fig. 3. Mlc1p localisation. (A) Mlc1-3HAp localisation after synchronous release from *cdc15-1* arrest, strain SSC218. At *t*=40 minutes staining is observed at the bud neck in late mitotic cells and at the incipient bud site in unbudded G_1 cells as indicated. Subsequently staining appears at the tip of growing buds, *t*=60 minutes. In early mitosis when the nucleus has moved to the bud site Mlc1-3HA staining occurs both in the bud tip and at the bud neck, *t*=80 minutes. At *t*=100 minutes cells are in mid to late mitosis and Mlc1-3HAp specific staining is observed at the bud neck in all cells. In a small proportion of these cells Mlc13HAp was also seen at the bud tip. In later time points staining is again observed at the early bud site and at the tip of small buds. In the right panels localised staining is highlighted by arrows. Bar, 10 μm. (B) Graphic representation of Mlc1-3HA staining at the bud neck contrasted with the binucleate index (i.e. late mitotic cells). The data demonstrate that at *t*=0 minutes all cells have Mlc1-3HAp st aining at the bud neck which rapidly disappears as cells undergo cytokinesis, *t*=60 minutes. By *t*=80 minutes the majority of cells exhibit bud neck staining and this precedes the peak in the number of binucleate cells by 20 minutes, indicative of localisation to the bud neck in early mitosis. Synchronous *cdc15-1* cells expressing Iqg1-3HAp were also fixed, stained with αHA and DAPI and 100 cells at each time point scored for the presence of Iqg1-3HA localisation at the bud neck and the binucleate index recorded. (C) Depletion of Mlc1p abolishes Iqg1p recruitment to the bud neck. SSC354 cells were released from G_0 into either galctose or glucose containing medium. After 6 hours Mlc1p was undetectable in cells grown in the presence of glucose. At this time point the majority cells had failed to complete cytokinesis and only 1% exhibited iqg1-3HAp staining at the bud neck. In contrast Iqg1-3HAp localised to the bud neck in 18% of control cells grown in galactose containing medium.

reminiscent of cells in which the Swe1p dependent G_2 morphology checkpoint has been activated (Lew and Reed, 1995). Given the involvement of Mlc1p in polarised cell growth we tested the appearance of this phenotype in a *swe1* deletion background. The results were similar to those shown in Fig. 2B with chains of multi-nucleate cells appearing at the same, late time points (data not shown), strongly suggesting that expression of GST-Mlc1p does not activate a *SWE1* dependent morphological checkpoint. In order to determine the localisation of GST-Mlc1p we performed immunofluorescence staining using an α-GST antibody. The fusion protein failed to localise to either the bud tip or bud neck, rather, it was found to be evenly distributed throughout mother and daughter cells (data not shown). These data are consistent with a dominant

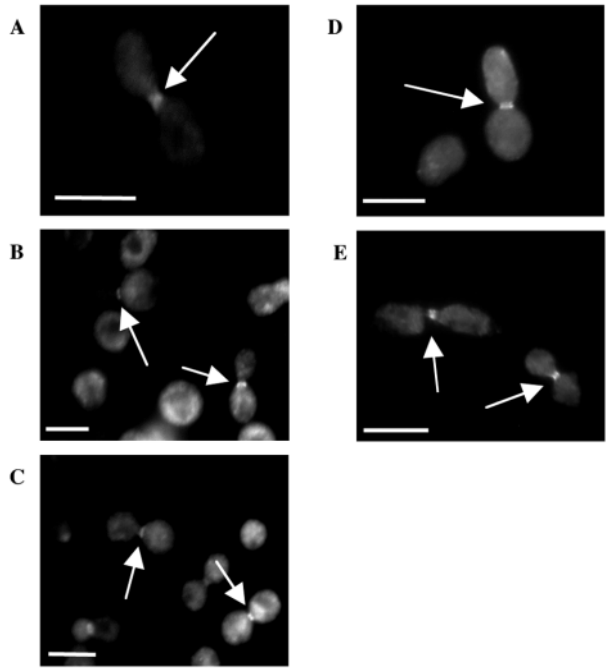

Fig. 4. Dependency of Mlc1p and Iqg1p localisation to the bud neck. Bars, 10 μm. Staining is indicated by arrows. (A) Maintenance of Mlc1p at the bud neck is independent of F-actin. Mlc1-3HAp, *cdc15-1* cells were arrested in late mitosis and treated with 200 μM LAT-A for 15 minutes prior to fixation and immuno-staining, strain SSC218. All late anaphase cells (96% of total cell number) exhibited Mlc1-3HAp staining at the bud neck. (B) Translocation of Mlc1p to the bud neck is independent of F-actin. Mlc1-3HAp expressing cells, SSC215, were arrested in S phase with HU and released in the presence of 200 μM LAT-A. Samples were taken at 20 minute intervals over 100 minutes. The cells shown were taken at *t*=40 minutes and processed for αHA immuno-staining; Mlc1-3HAp was found at the bud neck in 40% of cells at this time point compared to 44% of control cells released into DMSO containing medium in the absence of LAT-A. (C) Mlc1-3HAp localisation is independent of functional Iqg1p. Starvation synchronised *iqg1-1* cells expressing Mlc1-3HAp were released into fresh medium at 37°C, strain SSC216. The time course clearly shows αHA staining at the bud neck in mitotic cells (*t*=220 minutes) as indicated. (D) Mlc1-3HAp localisation is independent of Myo1p. A *myo1* deletion mutant expressing Mlc1-3HAp stains at the bud neck with αHA, strain SSC349. (E) Iqg1-3HAp localisation is independent of Myo1p. A *myo1* deletion mutant expressing Iqg1-3HAp stains at the bud neck with αHA, strain SSC350.

negative mechanism which involves the tiration of either Iqg1p or wild-type Mlc1p from the bud neck. High level expression of either GST or Mlc1p has no phenotypic effect indicating that the observed cytokinetic failure is a property of the fusion protein. We then tested whether actin and Iqg1-3HAp were able to localise to the bud neck when cytokinesis was inhibited by expression of the dominant negative GST-Mlc1p in asynchronous cultures. Despite repeated attempts we were unable to identify a single cell exhibiting actin or Iqg1-3HAp staining at the bud neck.

Depletion of Mlc1p prevents localisation of Iqg1p to the bud neck

SSC354 cells were released from G_0 into either glucose or galactose containing rich medium. Six hours after release into glucose Mlc1p was no longer detectable by western in comparison to cells released into galactose where Mlc1p protein was readily observed (Fig. 2C). At this time point 18% of galactose grown cells exhibited Iqg1-3HAp staining at the bud neck whilst only 1.4% of glucose grown cells showed similar staining (*n*=500, Fig. 2C). Taken together these data (Fig. 2B and C) strongly suggest that Mlc1p is required for the localisation of yeast IQGAP to the bud neck.

Cellular localisation of Mlc1p

Mlc1p was epitope tagged at the C terminus of the genomic locus using a PCR based targeted integration protocol (see Materials and Methods) and shown to be fully functional. Immunostaining of Mlc1-HA in both asynchronous (data not shown) and synchronous (Fig. 3A) cultures shows localisation to the growing bud and to the bud neck at mitosis. Manipulation of the focal plane demonstrates that Mlc1p clearly localises to a ring structure within the bud neck. Again the staining was specific as cells lacking the epitope tagged protein also lacked a fluorescent signal (data not shown). We often observed an apparent double ring structure at the bud neck, with one ring in each of the mother and daughter cells (e.g. Fig. 3A, *t*=100 minutes). In order to time the localisation of Mlc1p to these different sites we next analyzed the staining pattern in *cdc15-1* cultures synchronised at the restrictive temperature and subsequently released into fresh medium at 26°C (Fig. 3A). These data indicate that Mlc1p localizes to the incipient bud site in G_1 cells (*t*=40 minutes, Fig. 3A) then accumulates at the bud tip (*t*=60 minutes) before appearing at the bud neck at a point when there is a single nucleus situated at the bud neck (*t*=80 minutes). Therefore throughout the mitotic cell cycle Mlc1p is localised to sites of polar growth, only in G_0 cells do we fail to observe polarised localisation. Localisation at the bud neck is to the contractile ring structure and Mlc1p remains at this site as the ring undergoes contraction. The data are also presented graphically in order to emphasise the appearance of Mlc1p at the bud neck prior to anaphase as scored by the presence of two clearly divided nuclei (Fig. 3B). This experiment has been repeated on four separate occaisions with identical results. Iqg1p had previously been shown to localise to the bud neck late in the cell cycle (Epp and Chant, 1997; Lippincott and Li, 1998a). For comparison with Mlc1p we examined Iqg1-3HAp localisation in *cdc15-1* synchronised cultures. Iqg1-3HA is a fully functional C-terminal tagged version of Iqg1p encoded at the *IQG1* locus, see materials and methods for details. The results indicate that Iqg1-3HAp is first observed at the bud neck in mid-anaphase, slightly in advance of the appearance of fully binucleate cells (Fig. 3B) in broad agreement with the previous data. The localisation of Iqg1p in synchronous cultures has been repeated twice with same result. Four important points emerge from these data. Firstly localisation of Mlc1p to the presumptive bud site and the growing bud tip is similar to that of Myo2p. This result is consistent with a reported interaction between the two proteins (Brockerhoff et al., 1994; Lillie and Brown, 1994; Stevens and Davis, 1998). However, the localisation of Mlc1p at the bud neck in mitosis is distinct from Myo2p, occurring earlier in the cell cycle, which suggests the existence of alternative Mlc1p binding partners. Thirdly Mlc1p localisation to the bud neck precedes that of Iqg1p. Finally,

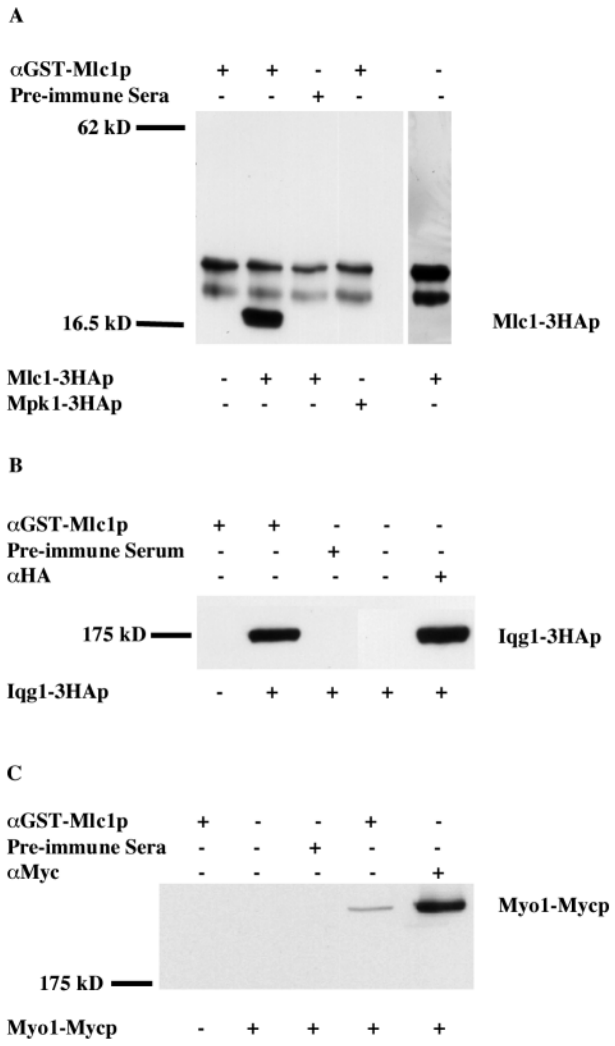

Fig. 5. Mlc1p and Iqg1p complex within the cell at mitosis. (A) Polyclonal anti-sera raised against GST-Mlc1p specifically immunoprecipitate Mlc1p. Western blot of an immunoprecipitation experiment probed with αHA. Lane 1, *cdc15-1* arrested cell extracts lacking the HA epitope precipitated with αGST-Mlc1p (strain SSC18). Lane 2, *cdc15-1* arrested cell extracts expressing Mlc1-3HAp precipitated with αGST-Mlc1p (strain SSC218). Lane 3, *cdc15-1* arrested cell extracts expressing Mlc1-3HAp precipitated with pre-immune serum (strain SSC218). Lane 4, cell extracts expressing Mpk1-3HA precipitated with αGST-Mlc1p. Lane 5 *cdc15-1* arrested cell extracts expressing Mlc1-3HAp precipitated in the absence of antibody (strain SSC218). Mlc1-3HA is precipitated by the polyclonal αGST-Mlc1p (lane 2) and not by pre-immune sera (lane 3). The antisera does not recognise control 59 kDa Mpk1-3HAp (lane 4) and does not precipitate αHA recognised polypeptides from an untagged control strain (lane 1). Two non-specific bands are apparent at 23 kDa and 28 kDa which are also present in Protein G bead precipitates in absence of immunoglobulins (lane 5). (B) Mlc1p and Iqg1p co-immunoprecipitation. Western blot developed with αHA. Lane 1, *cdc15-1* arrested cell extracts lacking Iqg1-3HAp precipitated with αGST-Mlc1p. Lane 2, *cdc15-1* arrested cell extracts expressing Iqg1-3HAp precipitated with αGST-Mlc1p (strain SSC226). Lane 3, *cdc15-1* arrested cell extracts expressing Iqg1-3HAp precipitated with pre-immune serum. Lane 4, *cdc15-1* arrested cell extracts expressing Iqg1-3HAp precipitated in the absence of antibody. Lane 5, *cdc15-1* arrested cell extracts expressing Iqg1-3HAp precipitated with αHA. Iqg1-3HAp is co-precipitated with Mlc1p by αGST-Mlc1p (lane 2) and not by pre-immune sera (lane 3) or in the absence of sera (lane 4). (C) Mlc1p and the class II myosin, Myo1p, co-immunoprecipitation. Western blot developed with αMyc. Lane 1, *cdc15-1* arrested cell extracts lacking Myo1-9Mycp precipitated with αGST-Mlc1p. Lane 2, *cdc15-1* arrested cell extracts expressing Myo1-9Mycp precipitated with Protein G Sepharose alone (strain SSC267). Lane 3, *cdc15-1* arrested cell extracts expressing Myo1-9Mycp precipitated with pre-immune serum. Lane 4, *cdc15-1* arrested cell extracts expressing Myo1-9Mycp precipitated in the with αGST-Mlc1p. Lane 5, *cdc15-1* arrested cell extracts expressing Myo1-9Mycp precipitated with αMyc. Myo1-9Mycp is co-precipitated with Mlc1p by αGST-Mlc1p (lane 4) and not by pre-immune sera (lane 3) or in the absence of sera (lane 2).

Mlc1p localisation to the bud neck must be independent of Iqg1p function and this is confirmed below (Fig. 4C).

Requirements for Mlc1p and Iqg1p localisation to the bud neck

The timing of Mlc1p localisation to the bud neck prompted us to examine the dependency of this upon several cytoskeletal elements. We first tested the requirement for filamentous actin for the maintenance of Mlc1p at the bud neck. Cells arrested in late anaphase were treated with actin depolymerising agent Latrunculin A (LAT-A) and subsequently examined by in situ immunofluorescence for Mlc1p localisation. Staining with rhodamine-conjugated phalloidin indicated that F-actin had been depolymerised (data not shown). Fig. 4A demonstrates that Mlc1p remains at the bud neck in the presence of LAT-A indicating that filamentous actin is not required for maintenance of Mlc1p at the bud neck. A second possibility is that F-actin is required for initial Mlc1p localisation to the bud neck but not for maintenance. Cells were synchronised in S phase with hydroxyurea (HU) and released in fresh, LAT-A, containing medium and then fixed at various time points. In the presence of HU only 7% of cells exhibit Mlc1-3HAp staining at the bud neck. Forty minutes after release Mlc1p is present at the bud neck in 39% of cells demonstrating that F-actin is not required for initial localisation to the bud neck (Fig. 4B). Mlc1p appearance at the bud neck precedes Iqg1p, predicting that localisation should be independent of *IQG1* function. In synchronised *iqg1-1* cells incubated at the restrictive temperature Mlc1p can clearly be seen at the bud neck (Fig. 4C) confirming the prediction.

The conventional myosin, Myo1p, is not absolutely required for cytokinesis and cells deleted for *myo1* are viable despite exhibiting cytokinetic defects of varying penetrance (Watts et al., 1987; Bi et al., 1998). Myo1p is known to localise to the presumptive bud site in early G_1 and to remain at the bud neck until cytokinesis is complete (Bi et al., 1998). One possibility is that Myo1p serves to recruit Mlc1p to the bud neck. The data shown in Fig. 4D and E demonstrate that both Mlc1p and Iqg1p are able to localise to the bud neck in the absence of Myo1p, ruling out this possibility.

The majority of proteins which localise to the bud neck require an intact septin ring (Field and Kellogg, 1999). We therefore examined Mlc1p and Iqg1p localisation in asynchronous *cdc12-1* cultures at both the permissive and restrictive temperatures. At the permissive temperature 33% of cells exhibited Mlc1-3HA staining at the bud neck and only 2% retained this staining following 120 minutes incubation at

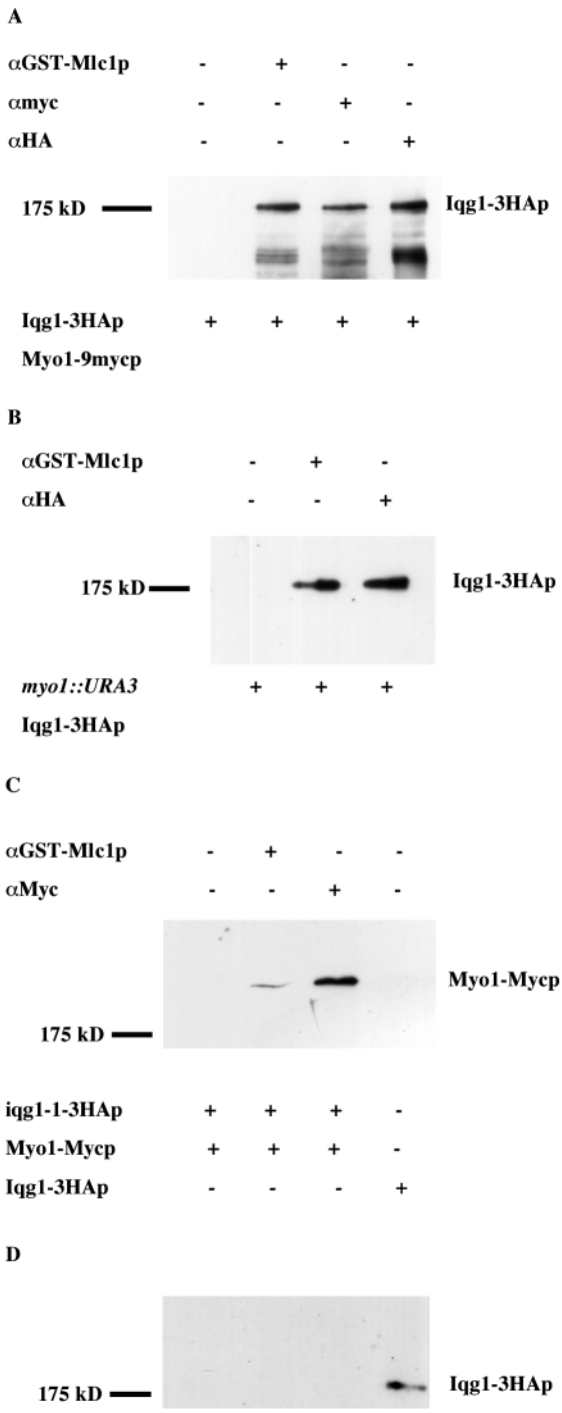

Fig. 6. Class II myosin and Iqg1p interact, although both form independent complexes with Mlc1p. (A) Western blot developed with αHA. Lane 1, *cdc15-1* arrested cell extracts expressing IQG1-3HAp and Myo1-9Mycp precipitated with Protein G Sepharose alone (strain SSC255). Lane 2, *cdc15-1* arrested cell extracts expressing IQG1-3HAp and Myo1-9Mycp precipitated with α-GST-MLC1p. Lane 3, *cdc15-1* arrested cell extracts expressing Iqg1-3HAp and Myo1-9Mycp precipitated with α-Myc. Lane 4, *cdc15-1* arrested cell extracts expressing Iqg1-3HAp and Myo1-9Mycp precipitated with α-HA. (B) Mlc1p and Iqg1p co-immunoprecipitate in the absence of class II myosin. Lane 1, *myo1* null mutant cells expressing Iqg1-3HAp precipitated with Protein G Sepharose alone (strain SSC350). Lane 2, *myo1* null mutant cells expressing IQG1-3HAp precipitated with α-GST-Mlc1p (strain SSC350). Lane 3, *myo1* null mutant cells expressing IQG1-3HAp precipitated with α-HA. (C) Mlc1p and Myo1p interaction does not require functional Iqg1p. Lane 1, *iqg1-1-3HA::TRP1* cells expressing Myo1-9Myc incubated for 3 hours at 37°C and precipitated with Protein G Sepharose alone (strain SSC351). Lane 2, *iqg1-1-3HA::TRP1* cells expressing Myo1-9Myc incubated for 3 hours at 37°C and precipitated with α-GST-MLC1p. Lane 3, *iqg1-1-3HA::TRP1* cells expressing Myo1-9Myc incubated for 3 hours at 37C and precipitated with αMyc. Lane 4, 100 μg of a total cell extract from cdc15-1 cells expressing Iqg1-3HAp arrested for 3 hours at 37°C (strain SSC226). (D) The filter from 6C, above, was stripped and then probed with αHA. It should be noted that all these experiments employed whole cell extracts from asynchronous cells and 5 mg of total soluble protein were used for the immunoprecipitations.

36°C. Similarly Iqg1p-3HA was found at the bud neck in 8% of cells at the permissive temperature and no specific bud neck staining was observed in cells shifted to the restrictive temperature for the same time period as before. In all cases 300 cells were scored. These data demonstrate that Mlc1p and Iqg1p localisation to the bud neck is septin dependent.

Mlc1p interacts with Iqg1p and Myo1p in late mitosis

The genetic relationship between *MLC1* and *IQG1* and co-localisation of Mlc1p and Iqg1p in mitosis are indicative of a physical interaction between the two proteins. We therefore performed co-immunoprecipitation experiments in order to establish whether or not such an interaction occurred. The data in Fig. 5A demonstrate the specificity of the GST-Mlc1p anti-sera showing that it recognizes MLC1-3HA in reciprocal immunoprecipitations. Polyclonal anti-GST-Mlc1p immunoprecipitates from mitotic extracts of a strain encoding Iqg1-3HAp contain single anti-HA reactive protein species of the appropriate mass, 174 kDa (Fig. 5B). Immunoprecipitation with either pre-immune sera or from a strain lacking Iqg1-3HAp does not identify a similar sized protein. A second candidate protein for Mlc1p interaction at the bud neck during cytokinesis is the conventional myosin encoded by *MYO1*. As shown in Fig. 5C Mlc1p and Myo1p interact in cells arrested in late mitosis at a point when all three proteins co-localise. We have not investigated the cell cycle dependency of these interactions.

Iqg1p and Myo1p form a complex

One question arising from the results described above and the fact that both proteins are members of the contractile ring (Bi et al., 1998; Lippincott and Li, 1998a) is whether or not Myo1p and Iqg1p can be isolated in a single complex. The data presented in Fig. 6A clearly demonstrate that epitope tagged Iqg1-3HAp can be co-precipitated with Myo1-9Mycp. Next we addressed whether Iqg1p and Myo1p form independent complexes with Mlc1p. In a *myo1* null mutant Mlc1p and Iqg1p retain the ability to form a complex as evidenced by co-immunoprecipitation (Fig. 6B). Similarly Myo1-9Mycp was precipitated with Mlc1p specific anti-sera in an *iqg1-1-3HA* strain following three hours incubation at the restrictive temperature, by which time more than 90% of the cells possessed multiple buds (Fig. 6C). It remained possible that the two proteins were complexed with the mutant Iqg1p. However, when the filter was stripped and re-probed with αHA no epitope tagged Iqg1p was evident in either the control

precipitation with α-GST-Mlc1p or that using Myo1p specific reagents (Fig. 6D). These data confirm that Iqg1p and the class II myosin reside within a single complex. However, Mlc1p forms distinct interactions with both proteins, presumably within the larger contractile ring structure.

DISCUSSION

Previous studies based on analysis of *iqg1* deletion mutants had identified a role for Iqg1p in cytokinesis and had localized the protein to the bud neck in mitosis (Lippincott and Li, 1998a; Epp and Chant, 1997). In contrast a third study implicated the protein in growth polarity and reported localisation of an Iqg1p fusion protein to the growing bud (Osman and Cerione, 1998). Here we have used a conditional mutation, termed *iqg1-1*, to analyse Iqg1p function more precisely in synchronous cultures. We observed normal polar bud growth and actin distribution in the first cycle followed by isotropic actin distribution and chitin deposition after several failed rounds of cytokinesis (Fig. 1A,B, and data not shown). We have also been able to localise wild-type levels of epitope tagged protein to the bud neck in late mitosis, as cells enter anaphase (Fig. 3B), but we have never observed polarised staining in the growing bud. The characterisation of the *iqg1-1* mutant phenotype is therefore consistent with the earlier two studies indicating a primary role for the protein in cytokinesis (Lippincott and Li, 1998a; Epp and Chant, 1997). The differences we observe from the third analysis may be attributable to the different genetic backgrounds. Alternatively the *iqg1-1* allele may disrupt cytokinesis but retain functions required for polarised growth. We also observe a failure of actin recruitment to the bud neck at the restrictive temperature which again is in agreement with the earlier work demonstrating the actin recruitment and binding properties of Iqg1p and its presence in the actomyosin contractile ring (Epp and Chant, 1997; Lippincott and Li, 1998a; Osman and Cerione, 1998; Shannon and Li, 1999).

We have identified *MLC1* as a dosage suppressor of the *iqg1-1* mutation (Fig. 2A). Suppression appears to be specific in that multi-copy *CMD1* does not permit growth at the restrictive temperature (Fig. 2A), despite the fact that calmodulin is reported to bind Iqg1p (Shannon and Li, 1999). Mlc1p localises to the incipient bud site in unbudded G_1 cells and to the growing bud tip before translocation to the bud neck at metaphase (Fig. 3A). These data are consistent with those of others demonstrating that Mlc1p binds to Myo2p and presumably acts as a regulatory light chain for that protein at sites of polarised growth (Stevens and Davis, 1998). However, *mlc1* null mutants exhibit a defect in Iqg1-3AHp localisation (Fig. 2C) and cytokinesis, which coupled to the *iqg1-1* suppression and localisation of the protein to the bud neck indicates that Mlc1p also functions during cytokinesis. Further an N-terminal GST-Mlc1p fusion protein acts in a dominant negative fashion to block cytokinesis but not polarized growth (Fig. 2B). There remain important questions relating to a role for Myo2p in cytokinesis and cell separation and its interaction with Cmd1p and Mlc1p. We have explored some of these issues and the data will be presented elsewhere, but the conclusions are that Myo2p plays no role in Mlc1p function in cytokinesis at or prior to acto-myosin ring contraction (J. R. Boyne and C. Price, unpublished).

Localisation of Mlc1p to the bud neck precedes that of Iqg1p and the latter protein fails to accumulate at the bud neck in mitosis when the dominant negative fusion protein is expressed. On the basis of these data together with the suppression data and the fact that Iqg1p requires the IQ domain to localise (Shannon and Li, 1999) we hypothesised that Mlc1p acts to recruit Iqg1p to the bud neck. This proposal predicts a physical interaction between Mlc1p and Iqg1p in mitosis and the data clearly demonstrate this interaction in cells blocked in late mitosis by the *cdc15-1* mutation (Fig. 5B). During the preparation of this manuscript similar data describing the localisation of Mlc1p and the interaction with Iqg1p were reported (Shannon and Li, 2000). Sequencing of the *iqg1-1* mutation revealed an amino acid substitution (L-P) at position 457. Analysis of the Iqg1p amino acid sequence predicts that L457 lies within a predicted α-helix (Rost and Sander, 1993) located in the centre of the IQ domain. By disruption of this helix the mutant protein may be rendered temperature sensitive for stability and/or Mlc1p binding. It is likely that increased concentration of Mlc1p rescues the temperature sensitivity of the mutated protein via a direct interaction. Recently a myosin essential light chain has been demonstrated to bind human IQGAP1 (Weissbach et al., 1998). Taken together with the data presented here it seems likely that myosin light chain interaction with IQGAP in cytokinesis has been conserved amongst eukaryotes.

We have also shown interaction between the conventional Class II myosin, Myo1p and Mlc1p at a late stage in mitosis. However, this interaction is not required for localisation of either the myosin light chain or Iqg1p to the bud neck (Fig. 4D and E). One issue that required clarification was whether the three proteins, Mlc1p, Iqg1p and Myo1p form a single complex or whether Mlc1p is bound separately to both Iqg1p and Myo1p. The data presented in Fig. 6 show that latter situation appears to be the case. That is, within the contractile ring Mlc1p forms distinct interactions with Myo1p and Iqg1p and probably does not form a bridge between the two proteins. These data lead us to propose a model in which Mlc1p localises to the bud neck in metaphase where it serves to recruit and then tether Iqg1p. Localisation of Mlc1p to the ring structure is entirely independent of the acto-myosin cytoskeleton and presumably requires interaction with an additional, as yet unknown, binding partner. Subsequently Mlc1p must bind Myo1p after which cytokinesis is triggered, by an as yet undetermined signal, leading to contraction of the acto-myosin ring.

A final consideration is why mutation of *iqg1* leads to a complete block in cytokinesis and lethality? Cells lacking Myo1p are able to complete cytokinesis albeit inefficiently and viability is not greatly reduced (Watts et al., 1987; Bi et al., 1998). Disruption of F-actin by LAT-A treatment also does not block cytokinesis (Ayscough et al., 1997; Bi et al., 1998). On the basis of these results it has been proposed that *S. cerevisiae* has two, partially redundant mechanisms for cytokinesis (Hales et al., 1999). Indeed other examples of eukaryotic cells undergoing cytokinesis in the absence of myosin II have been documented and this proposal may be extended to other organisms (reviewed by Field et al., 1999; Hales et al., 1999). Loss of either pathway then leads to a reduced efficiency of the process but only ablation of both pathways causes a terminal failure in cytokinesis. The simplest interpretation of *iqg1-1*

lethality is that Iqg1p is required for both of these pathways. Lethality may also reflect the multiple domain structure of Iqg1p. Failure to bind and thus correctly control the appropriate regulators and components of the actin cytoskeleton at cytokinesis may lead to secondary, pleiotropic effects on cell growth and regulation, which eventually leads to cell death.

We are grateful to Drs W. Zachariae and K. A. Nasmyth for providing the tagging vectors and to D. Stirling for the *CMD1* plasmid. We also thank Dr S. Smith (Sheffield Hybridomas) for his help in raising antisera. The work in Sheffield was funded by BBSRC, project grant 50/G10439, J.R.B is supported by a BBSRC research Studentship and H.M.Y. was in receipt of a graduate fellowship from Universiti Pertanian Malaysia. Work in Philadelphia was supported by grants from National Cancer Institute CA75954 and the March of Dimes Birth Defects Foundation.

REFERENCES

Adams, A. E. M. and Pringle, J. R. (1991). Staining of actin with fluorochrome conjugated phalloidin. *Meth. Enzymol.* **194**, 565-601.

Ayscough, K. R., Stryker, J., Pokala, N., Sanders, M., Crews, P. and Drubin, D. G. (1997). High rates of actin filament turnover and roles for actin in the establishment and maintenance of cell polarity revealed using actin inhibitor Latrunculin-A. *J. Cell Biol.* **137**, 399-416.

Ayscough, K. R. and Drubin, D. G. (1998). *Immunofluorescence Microscopy of Yeast Cells. Cell Biology: A Laboratory Handbook*. 2nd edn. Academic Press.

Bi, E., Maddox, P., Lew, D. J., Salmon, E. D., McMillan, J. N., Yeh, E. and Pringle, J. R. (1998). Involvement of an actomyosin contractile ring in *Saccharomyces cerevisiae* cytokinesis. *J. Cell Biol.* **142**, 1301-1312.

Bradford, M. M. (1976). A rapid and sensitive method for the quantitation of microgram quantities of protein utilizing the principle of protein-dye binding. *Anal. Biochem.* **72**, 248-254.

Brenner, C., Bieganowski, P., Pace, H. C. and Huebner, K. (1999). The histidine triad superfamily of nucleotide-binding proteins. *J. Cell. Physiol.* **181**, 179-187.

Brockerhoff, S. E., Stevens, R. C. and Davis, T. N. (1994). The unconventional myosin, Myo2p, is a calmodulin target at sites of cell growth in *Saccharomyces cerevisiae*. *J. Cell Biol.* **124**, 315-323.

Calvin, N. M. and Hanawalt, P. C. (1988). High-efficiency transformation of bacterial cells by electroporation. *J. Bacteriol.* **170**, 2796-2801.

Cheney, R. E. and Mooseker, M. S. (1992). Unconventional myosins. *Curr. Opin. Cell Biol.* **4**, 44-48.

Davis, T. N., Urdea, M. S., Masiarz, F. Z. and Thorner, J. (1986). Isolation of the yeast calmodulin gene: calmodulin is an essential protein. *Cell* **47**, 423-431.

Epp, J. A. and Chant, J. (1997). An IQGAP-related protein controls actin-ring formation and cytokinesis in yeast. *Curr. Biol.* **7**, 921-929.

Espindola, F. S., Espreafico, E. M., Coelho, M. V., Martins, A.R., Costa, F. R. C., Mooseker, M. S. and Larson, R. E. (1992). Biochemical and immunological characterization of p190-calmodulin complex from vertebrate brain: a novel calmodulin-binding myosin. *J. Cell Biol.* **118**, 359-368.

Field, C. M. and Kellogg, D. (1999). Septins: cytoskeletal polymers or signalling GTPases? *Trends Cell Biol.* **9**, 387-394.

Field, C., Li, R. and Oegema, K. (1999). Cytokinesis in eukaryotes: a mechanistic comparison. *Curr. Opin. Cell Biol.* **11**, 68-80.

Fromherz, S. and Szent-Gyorgi, A. G. (1995). Role of the essential light chain EF hand domains in calcium binding and regulation of scallop myosin. *Proc. Nat. Acad. Sci. USA* **92**, 7652-7656.

Glotzer, M. (1997). The mechanism and control of cytokinesis. *Curr. Opin. Cell Biol.* **9**, 815-819.

Govindan, B., Bowser, R. and Novick, P. (1995). The role of Myo2, a yeast class V myosin, in vesicular transport. *J. Cell Biol.* **128**, 1055-1068.

Hales, K. G., Bi, E., Wu, J-Q., Adam, J. C., Yu, I-C. and Pringle, J. R. (1999). Cytokinesis: an emerging unified theory for eukaryotes? *Curr. Opin. Cell Biol.* **11**, 717-725.

Harlow, E. and Lane, D. (1988). *Antibodies, A Laboratory Manual*. Cold Spring Harbor Press, New York.

Ito, H., Fukuda, Y., Murate, K. and Kimura, A. (1983). Transformation of intact yeast cells treated with alkali cations. *J. Bacteriol.* **153**, 163-168.

Johnston, G. C., Prendergast, J. A. and Singer, R. A. (1991). The *Saccharomyces cerevisiae MYO2* gene encodes an essential myosin for vectorial transport of vesiscles. *J. Cell Biol.* **113**, 539-551.

Kamei, T., Tanaka, K., Hihara, T., Umikawa, M., Imamura, H., Kikyo, M., Ozaki, K. and Takai, Y. (1998). Interaction of Bnr1p with a novel Src homology 3 domain-containing Hof1p. *J. Biol. Chem.* **273**, 28341-28345.

Kao, L.-R., Peterson, J., Ruiru, J., Bender, L. and Bender, A. (1996). Interactions between the ankyrin-repeat protein Akr1p and the pheromone response pathway in *Saccharomyces cerevisiae. Mol. Cell. Biol.* **16**, 168-178.

Keszenman-Pereyra, D. and Hieda, K. (1988). A colony procedure for transformation of *Saccharomyces cerevisiae*. *Curr. Genet.* **13**, 21-23.

Lew, D. J. and Reed, S. I. (1995). A cell cycle checkpoint monitors cell morphogenesis in budding yeast. *J. Cell Biol.* **129**, 739-749.

Lillie, S. H. and Brown, S. (1994). Immunofluorescence localization of the unconventional myosin, Myo2p, and the putative kinesin-related protein, Smy1p, to the same regions of polarised growth in *Saccharomyces cerevisiae*. *J. Cell Biol.* **125**, 825-842.

Lippincott, J. and Li, R. (1998a). Sequential assembly of myosin II, an IQGAP-like protein, and filamentous actin to a ring structure involved in budding yeast cytokinesis. *J. Cell Biol.* **140**, 355-366.

Lippincott, J. and Li, R. (1998b). Dual function of Cyk2, a cdc15/PSTPIP family protein, in regulating actomyosin ring dynamics and septin distribution. *J. Cell Biol.* **143**, 1947-1960.

Mitchell, D. A., Marshall, T. K. and Deschenes, R. J. (1993). Vectors for the inducible overexpression of glutathione S-transferase fusion proteins in yeast. *Yeast* **9**: 715-723.

Osman, M. A. and Cerione, R. A. (1998). Iqg1p, a yeast homologue of the mammalian IQGAPs, mediated Cdc42p effects on the actin cytoskeleton. *J. Cell Biol.* **142**, 443-455.

Philippsen, P., Stotz, A. and Scherf, C. (1991). DNA of *Saccharomyces cerevisiae. Meth. Enzymol.* **194**, 169-181.

Rose, M. D., Novick, P., Thomas, J. H., Botstein, D. and Fink, G. R. (1987). A *Saccharomyces cerevisiae* genomic plasmid bank based on a centromere-containing shuttle vector. *Gene* **60**, 237-243.

Rost, B. and Sander, C. (1993). Prediction of protein secondary structure at better than 70% accuracy. *J. Mol. Biol.* **232**, 584-599.

Shannon, K. B. and Li, R. (1999). The multiple roles of Cyk1p in the assembly and function of the actomyosin ring in budding yeast. *Mol. Biol. Cell* **10**, 283-296.

Shannon, K. B. and Li, R. (2000). A myosin light chain mediates the localisation of the budding yeast IQGAP-like protein during contractile ring formation. *Curr. Biol.* **10**, 727-730.

Sherman, F. (1991). Getting started with yeast. *Meth. Enzymol.* **194**, 3-20.

Smith, D. B. and Johnson, K. S. (1988). Single-step purification of polypeptides expressed in *Escherichia coli* as fusions with glutathione-S-transferase. *Gene* **67**, 31-40.

Stevens, R. C. and Davis, T. N. (1998). Mlc1p is a light chain for the unconventional myosin Myo2p in *Saccharomyces cerevisiae*. *J. Cell Biol.* **142**, 711-722.

Wach, A., Brachat, A., Pohlman, R. and Philippsen, P. (1994). New heterologous modules for classical or PCR-based gene disruptions in *Saccharomyces cerevisiae*. *Yeast* **10**, 1793-1808.

Watts, F. Z., Shiels, G. and Orr, E. (1987). The yeast *MYO1* gene encoding a myosin-like protein required for cell division. *EMBO J.* **6**, 3499-3505.

Weissbach, L., Bernards, A. and Herion, D. (1998). Binding of myosin essential light chain to the cytoskeletal-associated protein IQGAP1. *Biochem. Biophys. Commun*. **251**, 269-276.

Xie, X., Harrison, D. H., Schlichting, I., Sweet, R. M., Kalabokis, V. N., Szent-Gyorgyi, G. and Cohen, C. (1994). Structure of the regulatory domain of scallop myosin at 2.8A resolution. *Nature* **368**, 306-312.